

Photoelectrochemical Reduction of Carbon Dioxide on Quantum-Dot-Modified Electrodes by Electric Field Directed Layer-by-Layer Assembly Methodology

Diego Guzmán,[†] Mauricio Isaacs,^{*,†} Igor Osorio-Román,[†] Macarena García,[‡] Jason Astudillo,[‡] and Macarena Ohlbaum[†]

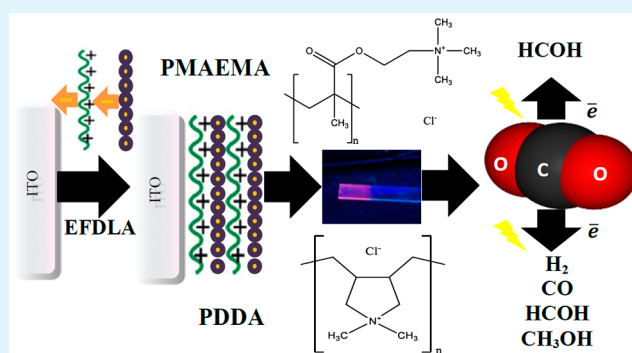
[†]Facultad de Química, Pontificia Universidad Católica de Chile, Vicuña Mackenna 4860, 7820436 Macul, Santiago, Chile

[‡]Facultad de Química y Biología, Universidad de Santiago de Chile, Libertador Bernardo O'Higgins 3363, 9170022 Santiago, Chile

Supporting Information

ABSTRACT: The photoelectrocatalytic reduction of CO₂ on ITO-modified electrodes, with electrostatic assemblies (polycations/quantum dots) (polycations = poly diallyldimethylammonium, PDDA, and poly(2-trimethylammonium)ethyl methacrylate, PMAEMA)), is described in the present work. Nanoparticles of CdTe (5.6 nm) were incorporated through an electric field directed layer-by-layer assembly method on ITO electrodes. Modified surfaces were active toward the reduction of CO₂ at -400 mV vs Ag/AgCl; the activity of ITO-(PMAEMA/QDs)₆ electrodes was enhanced by 300 mV under irradiation conditions. The photoelectrocatalytic effect was associated with the structure of the polycation and its influence in the assembly. Reaction products at -450 mV were H₂, CO, CH₃OH, and HCOH.

KEYWORDS: quantum dots, carbon dioxide, layer-by-layer, photoelectrochemical reduction, polycations



The rapid growth in energy demands during last century that resulted in a greater reliance on fossil fuels has generated an exponential increase in the concentration of carbon dioxide in the atmosphere by anthropogenic effect.¹ The efforts to minimize CO₂ emissions have focused on its reduction toward value-added products by the use of renewable energies and preferably under mild conditions of temperature and pressure, while also decreasing the high overpotential that exists in the electrochemical reduction of CO₂.²⁻⁴ The electro- and photoelectrochemical reduction of carbon dioxide has been carried out with semiconductor or metal particles, metalloporphyrins, phthalocyanines, and related macrocycles as molecular catalysts.³⁻⁸ The former has been widely explored in the recent decades, because p-type semiconducting electrodes can act as photocathodes for photoassisted CO₂ reduction.⁹

Considering the properties of quantum dots (QDs), such as their optoelectronic properties dependent on their size, shape, and composition,¹⁰ to explore their effect on the electro- and photoelectrochemical reduction of CO₂ is certainly of great interest. The use of different semiconductor nanocrystals in the catalytic and electrocatalytic oxidation of various compounds, such as chlorophenols,¹¹ dopamine,¹² sulfite,¹³ and methyl red,¹⁴ and in the reduction of benzene,¹⁴ nitrite,¹⁵ and carbon dioxide,^{14,16} have been previously reported. The incorporation of QDs on electrodic surfaces, mainly through the binding to the surface with different polymers or biomolecules, allows the

study of their photoelectrocatalytic properties and the effect of such binding. Indeed, a modified electrode with negatively charged QDs CdSe, incorporated as electrostatic assembly through a layer-by-layer method and poly diallyldimethylammonium (PDDA) as polycation, has been previously reported as sensors for the specific detection of Ramos cells.¹⁷ Other polycations, like poly allylamine (PAH), have been employed in layer-by-layer assemblies with CdTe nanocrystals.¹⁸ To the best of our knowledge, polycation poly(2-trimethylammonium) ethyl methacrylate (PMAEMA) has not been used in electrostatic assemblies with QDs.

Semiconductor bulk electrodes and quantum dots of the II-VIB groups, synthesized in organic solvents, have shown electrocatalytic activity toward the CO₂ reduction. In particular, the use of p-CdTe electrodes allowed the reduction of this molecule, resulting in the formation of useful carbon-based products such as CO, HCOOH and H₂ at -1160 mV vs Ag/AgCl in aqueous medium.^{9,16,19} However, the electrocatalytic activity of CdTe QDs, synthesized in aqueous medium and the effect of the polycation used in the assembly have not been previously investigated.

Received: June 26, 2015

Accepted: September 1, 2015

Published: September 1, 2015

CdTe QDs, with mercaptosuccinic acid (MSA) as capping agent, were prepared by a one-pot method in aqueous medium, following the procedure described in the [experimental methods](#). The size of the QDs was controlled with reflux time ([Figure S1](#)) and confirmed by transmission electron microscopy (TEM) and dynamic light scattering (DLS) ([Table S1](#)).²⁰ The characterization of the nanoparticles can be found in the [Supporting Information](#). For the study of the photoelectrocatalytic properties CdTe-MSA QDs of 5.6 nm were incorporated on ITO electrodes, following an electric field directed layer-by-layer assembly (EFDLA) method.²¹ Poly diallyldimethylammonium (PDDA) and poly(2-trimethylammonium) ethyl methacrylate methyl (PMAEMA) were used for the electrostatic assembly; the potential applied was 1000 mV.²¹ Although both are strong polycations, they present significant structural differences, cyclic vs branched monomer structures that could affect the assemblies in different ways, such as the type of growth mechanism and adsorption kinetics of the multilayers.²²

The growth of the electrostatic assemblies was monitored through UV-vis absorption spectroscopy ([Figure 1](#)). The

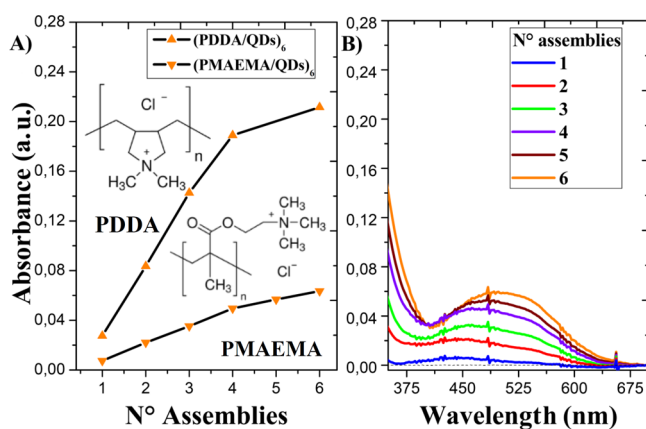


Figure 1. Growth of the (A) electrostatic assemblies and (B) (PMAEMA/QDs)₆ on the ITO electrode, monitored by UV-vis absorption, obtained by subtracting the baseline between each measurement. 5.6 nm CdTe-MSA QDs. Unmodified ITO baseline (---).

growth of an absorbance maximum peak, which increases with the number of bilayers to (Polycation/QDs)₆ was observed in both assemblies ([Figure 1 A](#)). A greater growth of the absorbance was observed with PDDA, while a smaller and more defined signal peak was observed with PMAEMA ([Figure 1 B](#)), both between 450 and 550 nm. These absorption bands can be correlated with the absorption peak shown by the QDs that is ascribed to the excitonic peak of the semiconductor ([Figure S1](#)).

Changes in the topography of the electrode, generated by the presence of the different polycations, were observed ([Figure 2](#)) comparing both surfaces by AFM. This is more evident when parameters such as height and surface roughness of the electrodes are considered ([Table S2](#)). The height of the surface increased from 12.7 nm on the ITO electrode to 212.6 and 183.5 nm on the modified electrodes with PDDA and PMAEMA, while the surface roughness (R_q) increased from 4.1 to 24.1 and 27.7 nm, respectively. Both features are related to the thickness of the film formed, supporting the effect of the polycation on the electrostatic assembly. In general, both modified electrodes showed nonuniform topographies with

homogeneous assemblies. When comparing electrostatic assemblies (PDDA/QDs)₆ and (PMAEMA/QDs)₆ the former presented a greater height, while the latter presents a greater roughness in average, which can be related to a greater presence of microdomain structures with the PMAEMA polycation. The smaller coefficient of roughness variation of the (PDDA/QDs)₆ assembly, 5.5 vs 26.7% of the (PMAEMA/QDs)₆, also indicates that the latter presents a more irregular surface.

The heterogeneous electrocatalytic properties of the modified electrodes were studied by j - E curves with the modified electrodes as working electrode and Pt and Ag/AgCl as counter and reference electrodes, under N₂ and CO₂ atmosphere. The photoelectrochemical properties for the CO₂ reduction were studied by applying white light (500 W Xe-Hg Lamp, Oriol Corporation). As it can be seen from [Figure 3 A, B](#), both modified electrodes were active in the electrochemical reduction of CO₂. With PDDA ([Figure 3 A](#)), a cathodic process with an onset potential at -200 mV in darkness was observed. Under irradiation, the cathodic process shift at -100 mV. A cathodic process starting at -300 mV in dark conditions was observed when PMAEMA was used ([Figure 3 B](#)). Under irradiation, the cathodic process started around 0 mV. These cathodic processes were not observed with ITO electrodes ([Figure S2](#)). The shift toward lower reduction potentials with light indicates the existence of electro and photoelectrocatalytic properties related to the reduction of CO₂. The bigger shift of the cathodic process with PMAEMA from darkness to irradiation conditions shows an important effect of the structure and size of the polycation on the packaging assembly.

The type of interaction of the polycation with the QDs in the electrostatic assembly can generate a small shift in the onset potential observed with both modified electrodes. PDDA functionalized carbon nanotubes electrodes, for example, were demonstrated as being capable of acting as metal-free catalyst for oxygen reduction reaction; shifts in their reduction potential were observed when modifications in the structure of the double layer changed the attractive interactions with oxygen, enhancing the intermolecular charge transfer and facilitating their electrocatalytic activity.²³ Depending on the potential range, for both assemblies, the cathodic current observed was higher or lower between darkness and irradiation conditions. In addition to the CO₂ reduction, electrochemical processes related to the hydrogen reduction could also be occurring under darkness conditions (pH 3.95).²⁴ Under irradiation conditions, the reactions related to the CO₂ reduction were promoted, reaching a plateau zone controlled by diffusion. At more negative potentials than -450 mV, this plateau was lower than the one observed in darkness. This could be due to the consumption of carbon dioxide in the double-layer region at lower potentials and the charge carriers recombination by the absence of an electron acceptor molecule (CO₂).²⁵

When comparing the number of electrostatic assemblies with the electrochemical response under CO₂ atmosphere ([Figure 3 A, B insets](#)), it can be seen a higher current at higher number of assemblies, associated with the structure and size of the polycation. An exponential and a linear increase were observed respectively in the PDDA electrode ([Figure 3A inset](#)) and in the PMAEMA electrode ([Figure 3B inset](#)). Moreover, when comparing such relationships under darkness irradiated conditions, similar responses were obtained with PDDA; however, important differences were obtained with PMAEMA. The greater photocurrent observed could be related to the

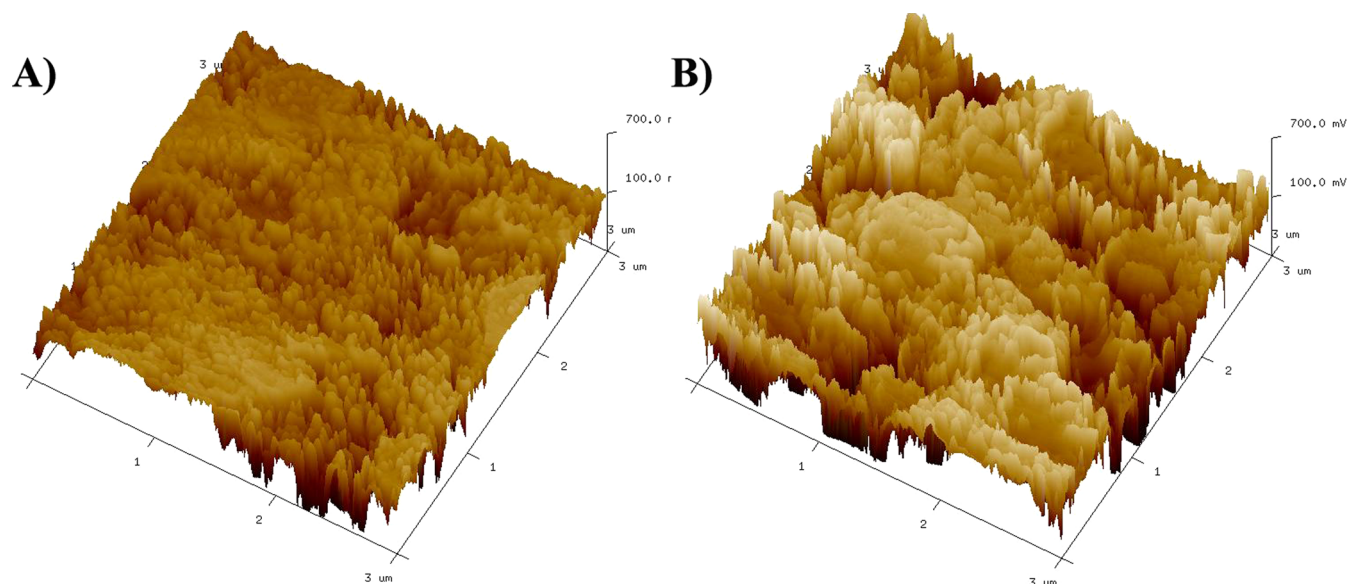


Figure 2. AFM phase imaging 3D of (A) ITO-(PDDA/QDs)₆ and (B) ITO-(PMAEMA/QDs)₆. CdTe-MSA QDs 5.6 nm. Size imaging 3 × 3 μm.

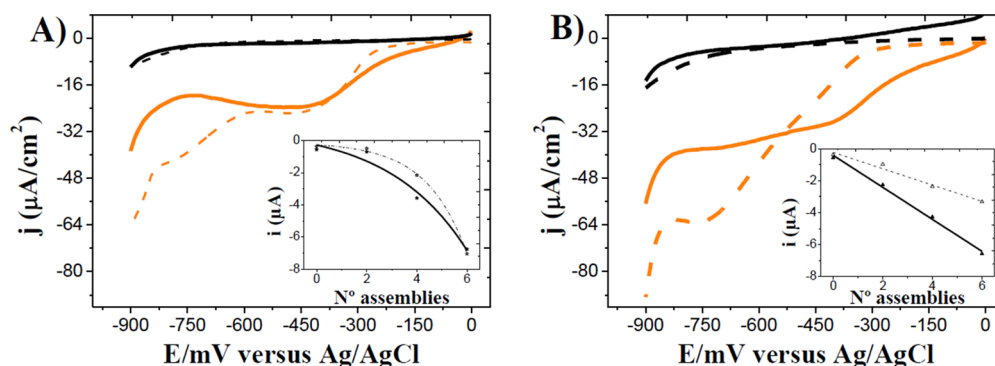


Figure 3. Curves j - E modified electrode ITO with assemblies (A) (PDDA/QDs)₆ and (B) (PMAEMA/QDs)₆ under N₂ (black) and CO₂ atmosphere (orange) in darkness (---) and white light (—). CdTe-MSA QDs 5.6 nm. Inset: Current intensity vs no. of assemblies under CO₂ atmosphere at -400 mV.

more irregular surface of the latter, which presents a more photoactive assembly where probably CO₂ molecule displays different adsorption modes enhancing subsequently light-induced charge transfer.⁹ Future electrochemical impedance spectroscopy (EIS) and in situ IR-ATR studies could give more information on the electrochemical behavior of the modified electrodes.²⁶

The products from the CO₂ reduction (Figure 4) were obtained through potential controlled electrolysis and its quantitative determination was carried out following UV-vis absorption spectroscopy and gas chromatography (GC). The time of electrolysis was 3 h and the applied potential was -450 mV. The products obtained with the (PDDA/QDs)₆ assembly were carbon monoxide, methanol and, in lesser amount, formaldehyde. Little difference between darkness and light conditions were observed, except for the additional generation of hydrogen under darkness, which could be related to the solvent reduction. On the other hand, only formaldehyde was observed with the (PMAEMA/QDs)₆ assembly. With PMAEMA, the effect of the white light applied on the electrode resulted in the production of more than twice the amount of HCOH obtained in the same conditions in darkness, showing again a greater effect of the light applied on the amount of product obtained when compared with the previous

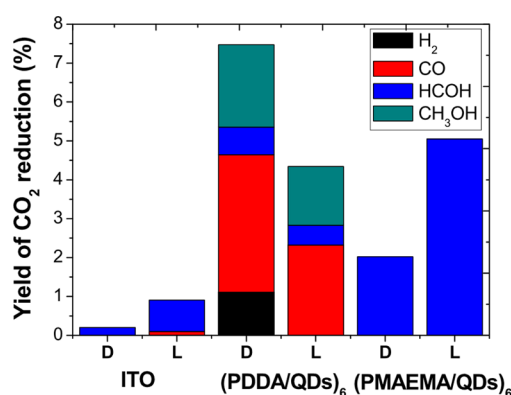


Figure 4. CO₂ reduction products obtained by potential controlled electrolysis in dark conditions (D) and light irradiation (L). Electrolysis time: 3 h. potential applied -450 mV. Yield calculated as a percentage of (μmol products/μmol nominal concentration CO₂).²⁷

results. This highlighted the importance of the electrostatic assembly on their photoelectrocatalytic properties.² The products confirmed the reduction of CO₂ with the modified

electrodes, also presenting the possibility of carrying out selective reduction process depending on the polycation.

Comparing the amount of products obtained with the different assemblies, the more irregular surface of the assembly (PMAEMA/QDs)₆ largely affects the heterogeneous charge-transfer process under darkness and irradiation conditions. The different products obtained with both assemblies could be attributed to changes in the interaction between the polycations and the QDs, explained before,²³ and the CO₂ molecules, caused by their dissimilar surface structures and resulting in two proposed reduction pathways mechanisms: formaldehyde and carbene pathways.²⁸ These possible reduction mechanisms were studied mainly in TiO₂; the binding of the activated CO₂ molecule through one of its atoms to the titanium atom follows a formaldehyde pathway, whereas the binding through two oxygen atoms to two titanium atoms results in a carbene pathway. In both mechanisms, the products obtained were intermediate species or one of the final products of either reduction mechanism. The main products obtained with the ITO-(PDDA/QDs)₆ electrode were carbon monoxide and methanol, which could be correlated to a carbene pathway, whereas the product obtained with the ITO-(PMAEMA/QDs)₆ electrode could be correlated the formaldehyde pathway.²⁸

In summary, it was possible to modify ITO electrodes with assemblies (polycations/QDs), with polycations PDDA and PMAEMA, confirming it through UV-vis absorption spectroscopy and AFM imaging. Electrostatic assemblies with PDDA and PMAEMA and QDs of the same size (5.6 nm) exhibit cathodic process, in CO₂ saturated solution, between -200 and -100 mV with PDDA, and between -300 and 0 mV with PMAEMA in darkness and white light, respectively, confirming the existence of electro- and photoelectrocatalytic effects against CO₂ with the modified electrodes. Polycations with different monomer structures generate different arrangements in the assemblies, which can limit the effects of light on the QDs photoelectrocatalytic properties. Through potential controlled electrolysis, the reduction of CO₂ was confirmed with the modified electrodes, with (PMAEMA/QDs)₆ assemblies being more selective toward the production of HCOH.

EXPERIMENTAL METHODS

CdTe-MSA QDs were synthesized following a "one-pot" method in aqueous medium, based on the conditions described on as a protocol developed by our research group.²¹ All reactions were carried out in 50 mL of a solution with 0.015 M Na₂B₄O₇ and 0.015 M citrate (pH 7.0). Then 1 mM CdCl₂, 0.25 mM Na₂TeO₃, and 3 mM mercaptosuccinic acid (MSA) were added and the solution was stirred vigorously for 5 min. Finally, 0.012 M NaBH₄ were added and the solution was incubated at 90 °C. The size of the nanoparticles was controlled with the reflux time.

The electrostatic assembly was prepared on the ITO electrode following literature procedures,^{17,21} by an electric field layer-by-layer directed assembly method (EFDLA). First, the ITO electrodes were sonicated in acetone, 1 M NaOH, 1:1 (v/v) ethanol/water and water respectively, for 15 min each. After that, the (polycation/QDs)_n assembly was grown by alternately immersion of the surface on solutions of 0.0756 mM Polycation ((polycation = poly diallyldimethylammonium, PDDA, or poly(2-trimethylammonium) ethyl methacrylate methyl, PMAEMA)) and 0.5 M NaCl. The layer-by-layer, supported by electrophoretic deposition, was performed in a one-compartment system with two ITO electrodes, a working electrode (modified electrode), and a counter electrode, with an applied potential of 1000 mV for 5 min. The process was repeated to obtain a

desired number of (polycation/QDs)_n assemblies. Between each step, the surface was rinsed with H₂O mili-Q and dried at room temperature.

Nanoparticle and electrostatic assembly growth was monitored by UV-vis spectroscopy, with a Shimadzu Multispec 1501 spectrophotometer. The size of the nanoparticles and their size-distribution was determined by a Philips Tecnai 12 BioTwin (Eindhoven, The Netherlands) TEM microscope and dynamic light scattering (DLS) technique, with Zetasizer Nano ZS, respectively. The morphological properties of the modified electrodes were studied using a Bruker Nanoscope Innova AFM microscope.

The studies of the electro and photoelectrochemical reduction of CO₂ were carried out in three-electrode systems, using the modified ITO, Ag/AgCl and Pt as the working, reference and counter electrodes, respectively. All electrochemical measurements were performed with a potentiostat BASI 50CV-W and carried out in 0.1 M NaClO₄ electrolyte solution. Previously, the electrolyte solution was saturated with N₂ and subsequently with CO₂ at room temperature. The CO₂ reduction was studied by *j*-*E* curves, obtained with a linear sweep voltammetry (LSV) technique, between 0 and -900 mV and a scan rate of 5 mV/s. The controlled-potential electrolysis was carried out in a gastight H-type cell with an Agar-KCl_(sat) salt bridge and a BASI POWER MODULE PWR-3 potentiostat; the applied potential was -450 mV, during 3 h. The photoelectrochemical studies were carried out using the same systems, irradiated with light provided by a 500 W xenon-mercury lamp system (Oriol Co). The analysis of products was made using UV-vis spectroscopic methods reported in literature.²⁹ The gaseous products were analyzed with a DANI Master gas chromatograph (GC), with a micro thermal conductivity (μ TCD) and a flame ionization (FID) detector² with Molecular Sieves and Carbowax capillary columns, respectively.

ASSOCIATED CONTENT

Supporting Information

The Supporting Information is available free of charge on the ACS Publications website at DOI: 10.1021/acsami.5b05722.

UV-vis absorption and emission spectra of the quantum dots CdTe-MSA synthesized, as well as the size characterization of the QDs by TEM and DLS (PDF)

AUTHOR INFORMATION

Corresponding Author

*E-mail: misaacs@uc.cl.

Notes

The authors declare no competing financial interest.

ACKNOWLEDGMENTS

This work was supported by Project RC 130006, CILIS, granted by Fondo de Innovación para la Competitividad, del Ministerio de Economía, Fomento y Turismo, Chile, and FONDECYT 1141199, CONICYT 21120437 grant, and Pontificia Universidad Católica de Chile.

REFERENCES

- (1) Grace, A. N.; Choi, S. Y.; Vinoba, M.; Bhagiyalakshmi, M.; Chu, D. H.; Yoon, Y.; Nam, S. C.; Jeong, S. K. Electrochemical Reduction of Carbon Dioxide at Low Overpotential on a Polyaniline/Cu₂O Nanocomposite Based Electrode. *Appl. Energy* **2014**, *120*, 85–94.
- (2) García, M.; Aguirre, M. J.; Canzi, G.; Kubiak, C. P.; Ohlbaum, M.; Isaacs, M. Electro and Photoelectrochemical Reduction of Carbon Dioxide on Multimetallic Porphyrins/Polyoxotungstate Modified Electrodes. *Electrochim. Acta* **2014**, *115*, 146–154.
- (3) Liu, Q.; Wu, D.; Zhou, Y.; Su, H.; Wang, R.; Zhang, C.; Yan, S.; Xiao, M.; Zou, Z. Single-Crystalline, Ultrathin ZnGa₂O₄ Nanosheet Scaffolds to Promote Photocatalytic Activity in CO₂ Reduction into Methane. *ACS Appl. Mater. Interfaces* **2014**, *6*, 2356–2361.

- (4) Zhao, H.; Zhang, Y.; Zhao, B.; Chang, Y.; Li, Z. Electrochemical Reduction of Carbon Dioxide in an MFC–MEC System with a Layer-by-Layer Self-Assembly Carbon Nanotube/Cobalt Phthalocyanine Modified Electrode. *Environ. Sci. Technol.* **2012**, *46*, 5198–5204.
- (5) Inglis, J. L.; MacLean, B. J.; Pryce, M. T.; Vos, J. G. Electrocatalytic Pathways Towards Sustainable Fuel Production from Water and CO₂. *Coord. Chem. Rev.* **2012**, *256*, 2571–2600.
- (6) Yui, T.; Tamaki, Y.; Sekizawa, K.; Ishitani, O. Photocatalytic Reduction of CO₂: From Molecules to Semiconductors. In *Photocatalysis*; Bignozzi, C. A., Ed.; Springer-Verlag: Berlin, 2011; Vol. 303, pp 151–184.
- (7) Isaacs, M.; Armijo, F.; Ramírez, G.; Trollund, E.; Biaggio, S. R.; Costamagna, J.; Aguirre, M. J. Electrochemical Reduction of CO₂ Mediated by Poly-M-aminophthalocyanines (M = Co, Ni, Fe): Poly-Co-tetraaminophthalocyanine, a Selective Catalyst. *J. Mol. Catal. A: Chem.* **2005**, *229*, 249–257.
- (8) Isaacs, M.; Canales, J. C.; Aguirre, M. J.; Costamagna, J. Contribution of the Ligand on the Electroreduction of CO₂ Catalyzed by a Cobalt (II) Macrocyclic Complex. *J. Coord. Chem.* **2003**, *56*, 1193–1201.
- (9) Kumar, B.; Llorente, M.; Froehlich, J.; Dang, T.; Sathrum, A.; Kubiak, C. P. Photochemical and Photoelectrochemical Reduction of CO₂. *Annu. Rev. Phys. Chem.* **2012**, *63*, 541–569.
- (10) Amelia, M.; Lincheneau, C.; Silvi, S.; Credi, A. Electrochemical Properties of CdSe and CdTe Quantum Dots. *Chem. Soc. Rev.* **2012**, *41*, 5728–5743.
- (11) Khene, S.; Nyokong, T. Redox Activity of CdTe Quantum Dots Linked to Nickel Tetraaminophthalocyanine: Effects of Adsorption Versus Electrodeposition on the Catalytic Oxidation of Chlorophenols. *Microchem. J.* **2011**, *99*, 478–485.
- (12) Hao, Q.; Wang, P.; Ma, X.; Su, M.; Lei, J.; Ju, H. Charge Recombination Suppression-based Photoelectrochemical Strategy for Detection of Dopamine. *Electrochem. Commun.* **2012**, *21*, 39–41.
- (13) Raevskaya, A. E.; Stroyuk, A. L.; Kuchmii, S. Y. CdS Nanoparticle Photocatalysis of the Chain Oxidation of Sulfite Ions by Molecular Oxygen. *Theor. Exp. Chem.* **2003**, *39*, 235–241.
- (14) Kang, Z.; Tsang, C. H. A.; Wong, N.-B.; Zhang, Z.; Lee, S.-T. Silicon Quantum Dots: A General Photocatalyst for Reduction, Decomposition, and Selective Oxidation Reactions. *J. Am. Chem. Soc.* **2007**, *129*, 12090–12091.
- (15) Ranjit, K. T.; Viswanathan, B. Photoelectrochemical Reduction of Nitrite Ions to Ammonia on CdS Photocatalysts. *J. Photochem. Photobiol., A* **2003**, *154*, 299–302.
- (16) Wang, L. G.; Pennycook, S. J.; Pantelides, S. T. The Role of the Nanoscale in Surface Reactions: CO₂ on CdSe. *Phys. Rev. Lett.* **2002**, *89*, 1–4.
- (17) Zhang, X.; Li, S.; Jin, X.; Li, X. Aptamer Based Photoelectrochemical Cytosensor with Layer-by-layer Assembly of CdSe Semiconductor Nanoparticles as Photoelectrochemically Active Species. *Biosens. Bioelectron.* **2011**, *26*, 3674–3678.
- (18) Chapel, J.-P.; Berret, J.-F. Versatile Electrostatic Assembly of Nanoparticles and Polyelectrolytes: Coating, Clustering and Layer-by-layer Processes. *Curr. Opin. Colloid Interface Sci.* **2012**, *17*, 97–105.
- (19) Yoneyama, H.; Sugimura, K.; Kuwabata, S. Effects of Electrolytes on the Photoelectrochemical Reduction of Carbon Dioxide at Illuminated P-type Cadmium Telluride and P-type Indium Phosphide Electrodes in Aqueous Solutions. *J. Electroanal. Chem. Interfacial Electrochem.* **1988**, *249*, 143–153.
- (20) Díaz, V.; Ramírez-Maureira, M.; Monrás, J. P.; Vargas, J.; Bravo, D.; Osorio-Román, I. O.; Vásquez, C. C.; Pérez-Donoso, J. M. Spectroscopic Properties and Biocompatibility Studies of CdTe Quantum Dots Capped with Biological Thiols. *Sci. Adv. Mater.* **2012**, *4*, 1–8.
- (21) Gao, M.; Sun, J.; Dulkeith, E.; Gaponik, N.; Lemmer, U.; Feldmann, J. Lateral Patterning of CdTe Nanocrystal Films by the Electric Field Directed Layer-by-Layer Assembly Method. *Langmuir* **2002**, *18*, 4098–4102.
- (22) Guzmán, E.; Ritacco, H. A.; Ortega, F.; Rubio, R. G. Growth of Polyelectrolyte Layers Formed by Poly(4-styrenesulfonate sodium salt) and Two Different Polycations: New Insights from Study of Adsorption Kinetics. *J. Phys. Chem. C* **2012**, *116*, 15474–15483.
- (23) Wang, S.; Yu, D.; Dai, L. Polyelectrolyte Functionalized Carbon Nanotubes as Efficient Metal-free Electrocatalysts for Oxygen Reduction. *J. Am. Chem. Soc.* **2011**, *133*, 5182–5185.
- (24) Remita, E.; Tribollet, B.; Sutter, E.; Vivier, V.; Ropital, F.; Kittle, J. Hydrogen Evolution in Aqueous Solutions Containing Dissolved CO₂: Quantitative Contribution of the Buffering Effect. *Corros. Sci.* **2008**, *50*, 1433–1440.
- (25) Ogura, K.; Ferrell, J. R.; Cugini, A. V.; Smotkin, E. S.; Salazar-Villalpando, M. D. CO₂ Attraction by Specifically Adsorbed Anions and Subsequent Accelerated Electrochemical Reduction. *Electrochim. Acta* **2010**, *56*, 381–386.
- (26) Jie, G.; Li, L.; Chen, C.; Xuan, J.; Zhu, J.-J. Enhanced Electrochemiluminescence of CdSe Quantum Dots Compositing with CNTs and PDDA for Sensitive Immunoassay. *Biosens. Bioelectron.* **2009**, *24*, 3352–3358.
- (27) Schneider, J.; Jia, H.; Muckerman, J. T.; Fujita, E. Thermodynamics and Kinetics of CO₂, CO, and H⁺ Binding to the Metal Centre of CO₂ Reduction Catalysts. *Chem. Soc. Rev.* **2012**, *41*, 2036–2051.
- (28) Habisreutinger, S. N.; Schmidt-Mende, L.; Stolarczyk, J. K. Photocatalytic Reduction of CO₂ on TiO₂ and Other Semiconductors. *Angew. Chem., Int. Ed.* **2013**, *52*, 7372–7408.
- (29) Dreyse, P.; Isaacs, M.; Calfumán, K.; Cáceres, C.; Aliaga, A.; Aguirre, M. J.; Villagra, D. Electrochemical Reduction of Nitrite at Poly-[Ru(5-NO₂-phen)₂Cl] Tetrapyrrolyl Porphyrin Glassy Carbon Modified Electrode. *Electrochim. Acta* **2011**, *56*, 5230–5237.